Free-Strain Consolidation of Soft Ground Improved with Alternating Length PVDs

Bowen Lv[1], Chen Zhang[1], Weihong Zhou[1], Fei Wang[1], Hao Wang[1] and Zheng Chen[2,*]

[1] The Third Construction Co., Ltd. of China Construction Eighth Engineering Division, Nanjing, 210023, China

[2] School of Civil Engineering and Architecture, Hainan University, Haikou, 570228, China

INFORMATION

Keywords:
Alternating length PVDs
model equivalence
mixed-type boundary
boundary transform method
local discretization
average degree of consolidation

DOI: 10.23967/j.rimni.2025.10.65700

SCIPEDIA Revista Internacional de Métodos Numéricos para Cálculo y Diseño en Ingeniería

RIMNI Revista Internacional Métodos numéricos para cálculo y diseño en ingeniería

Free-Strain Consolidation of Soft Ground Improved with Alternating Length PVDs

Bowen Lv[1], Chen Zhang[1], Weihong Zhou[1], Fei Wang[1], Hao Wang[1] and Zheng Chen[2,*]

[1]The Third Construction Co., Ltd. of China Construction Eighth Engineering Division, Nanjing, 210023, China

[2]School of Civil Engineering and Architecture, Hainan University, Haikou, 570228, China

ABSTRACT

In practice, installation of alternating length prefabricated vertical drains (PVDs) cannot only satisfy the strength requirements for the upper soil layer, but also improve the lower soil layer to a certain extent, which is conducive to improving the overall strength and stability of the ground. In this paper, the original three-dimensional consolidation model for alternating length PVDs is simplified into a plane equivalent model, considering only well resistance by the model equivalence technique. Subsequently, a novel semi-analytical solution for soft ground with alternating length PVDs is derived using the boundary transform and local discretization methods. Accuracy analysis of local discretization is conducted to determine the appropriate segment number for PVD-soil interface boundaries. The effectiveness of the proposed solution is demonstrated by comparing the results from numerical analyses. Finally, the influence of the penetration depth of short and long PVDs on the consolidation efficiency is studied. Results show that the installation of alternating length PVDs is more effective compared to the conventional scheme of equal length installation. Both the average degrees of consolidation within and below a design depth for the ground with alternating length PVDs are higher than in the case with equal length PVDs.

OPEN ACCESS

Received: 20/03/2025

Accepted: 22/05/2025

Published: 14/07/2025

DOI
10.23967/j.rimni.2025.10.65700

Keywords:
Alternating length PVDs
model equivalence
mixed-type boundary
boundary transform method
local discretization
average degree of consolidation

1 Introduction

Prefabricated vertical drains (PVDs) are essential in ground improvement strategies, particularly for infrastructure projects such as roadways, embankments, and foundations. While equal-length PVDs are typically employed, this approach is often not cost-effective for deep soft soil foundations. Existing consolidation theories primarily address soft ground stabilized with equal-length PVDs, leaving the consolidation behavior of soft ground treated with unequal-length PVDs underdeveloped. The alternating-length layout, a commonly used configuration for PVDs of unequal length, has demonstrated promising results in practice [1]. Therefore, developing a consolidation model for soft ground treated with alternating length PVDs is crucial to bridging this knowledge gap.

*Correspondence: Zheng Chen (geozhengchen@gmail.com). This is an article distributed under the terms of the Creative Commons BY-NC-SA license

Based on the equal strain assumption, Barron [2] established the consolidation theory of the ground with fully penetrating vertical drains for the first time. However, his solution can only satisfy the governing equation at the initial time (i.e., $t = 0$) when the well resistance is considered. Hansbo [3] simplified this consolidation theory and provided a widely used approximate solution that has a clear physical meaning. To improve the consolidation theory of the ground with fully penetrating vertical drains, Xie and Zeng [4] established an accurate solution satisfying the governing equation and all solving conditions based on the work of Hansbo [3]. Subsequently, numerous scholars have since extended these theories, including models that consider time-dependent loading [5–8], multilayered soils [6,9–11], time-dependent well resistance [12–14], non-Darcian flow [15–18], large strain [18,19], and so on.

Partially penetrating PVDs also belong to equal-length PVDs due to the same length of each PVD. Equal length PVDs must be partially penetrated when the soft soil layer is too thick, the bottom of the soil layer is pervious to cause the loss of vacuum pressure, or the vertical applied load is not high enough to justify the full penetration of PVDs into the entire clay layer [20]. As for the consolidation of the ground with partially penetrating equal-length PVDs, Hart et al. [21] calculated the radial and vertical consolidation, respectively, and obtained an approximate solution for the overall average degree of consolidation by combining the radial and vertical consolidation. To accurately reflect the three-dimensional characteristics of the consolidating soil, Tang and Onitsuka [10] considered both radial and vertical seepage flow in the improved layer, whereas consolidation of the underlying layer was still assumed to be one-dimensional. This measure is still used in subsequent works on the consolidation behavior of the ground with partially penetrating PVDs [22]. However, the consolidation of the underlying layer is three-dimensional, especially in the area near the bottom of PVDs. Given this, Wang and Jiao [23] introduced the concept of virtual vertical drain, that is, the soil directly below the PVD can be regarded as a virtual vertical drain with the same properties of the underlying soil, to convert the consolidation problem of the ground with partially penetrating PVDs into the response of a double-layered ground with fully penetrating PVDs. In summary, the solutions in these studies are based on the equal strain assumption, and the solving procedures are very complex, losing the original intention of simplifying the consolidation calculation. In addition, compared with the equal strain assumption, the free strain assumption is more in line with the actual engineering situation. Given this, Chen et al. [24] proposed a semi-analytical solution for soil consolidation with partially penetrating PVDs under free-strain conditions.

All consolidation theories mentioned above are limited to analyzing the ground improved with equal-length PVDs. When a thick, soft soil layer is encountered, installation of long equal-length PVDs is not cost-effective, while the use of short equal-length PVDs cannot meet the design requirements for the underlying layer, resulting in potential safety issues in practice. Hence, the approach of alternating length PVDs that combines the advantages of short and long PVDs is proposed. On the one hand, the design requirements for the upper soil layer can be met through both short and long PVDs. On the other hand, the lower soil layer is improved through long PVDs, which is conducive to the overall strength and stability of the ground. However, research on the consolidation of the ground with alternating length PVDs is lacking, resulting in no theoretical support for engineering design.

The main purpose of this work is to obtain a semi-analytical solution for free strain consolidation of the ground with alternating length PVDs. Firstly, the original three-dimensional consolidation model is converted into a plane consolidation model using the model equivalence technique. Then, the solution of the equivalent plane model is obtained using the boundary transform and local discretization methods. After the effectiveness of the proposed solution is evaluated against numerical simulation, the sensitivity of the penetration depth of PVDs is analyzed in detail.

2 Model Description and Equivalence

2.1 Model Description

Fig. 1 depicts a surcharge preloading system with alternating length PVDs for ground improvement. The same type of PVDs with varying lengths are alternately installed in a square pattern, with short PVDs always located in the middle of four adjacent long PVDs (the spacing between adjacent short or long PVDs is denoted by d). The PVD has an equivalent radius of r_w^o and a vertical permeability of k_w^o. The penetration depths for short and long PVDs are denoted by L^s and L^l (L^s and L^l do not exceed the thickness of the ground, H), respectively. Installation of each PVD could form a smear zone with a radius of r_s^o and a horizontal permeability of k_s^o. The undisturbed zone has a horizontal permeability of k_h^o, a vertical permeability k_v^o, and a volumetric compressibility of m_v^o. In addition, a surcharge loading, $\sigma(t)$, is applied to the ground surface.

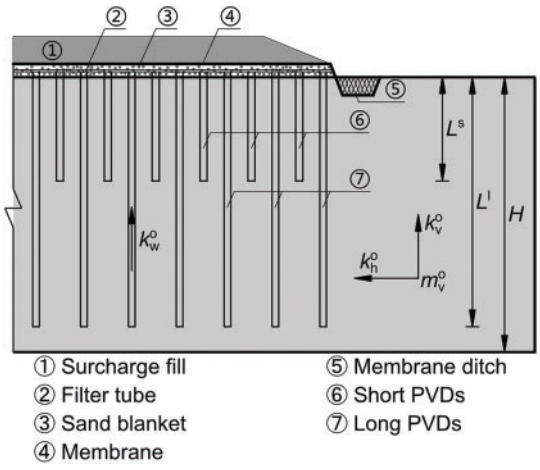

Figure 1: Schematic diagram of a surcharge preloading system with alternating long-short PVDs for ground improvement

2.2 Model Equivalence

For the ground improved with equal-length PVDs, a unit cell is typically adopted based on the spatial symmetry method in the cylindrical coordinate system proposed by Barron [2]. However, when short and long PVDs are alternately installed in the ground, the non-uniform lengths of PVDs prevent the establishment of the seepage symmetry plane required for extracting an axisymmetric unit cell for the consolidation analysis in the cylindrical coordinate system. To address this problem, this study adopts the plane consolidation model as an equivalent substitute for the original three-dimensional model [25–27]. This approach is frequently employed to replace the original three-dimensional model for numerical calculations due to its better computational efficiency [28–30].

To simplify the consolidation model, the original model is divided into two parts: one part with only short PVDs and another part with only long PVDs (see Fig. 2a). Each column (or row) of PVDs in these two parts is converted into an equivalent drain wall independently using the method proposed by Liu and Shi [25] (see Fig. 2b and c). The distance between adjacent drain walls is set as d to ensure a successful combination of the two equivalent parts. A unit cell, as shown in Fig. 2c, is extracted for consistency calculation based on the geometric symmetry of the combined plane model. It should be noted that following the model transformation, only the half-width of drain wall (b_w) and the equivalent horizontal permeability (k_h) are adjusted, and the parameters k_s^o and r_s^o characterizing the smear effect are incorporated into the equivalent parameter k_h (For the detailed

equivalence procedure, refer to Supplementary Materials). In addition to the geometric parameters L^{s}, L^{l}, and H, all other parameters—including the equivalent vertical ground permeability (k_{v}), equivalent volumetric compressibility of the ground (m_{v}), and equivalent vertical permeability of the drain wall (k_{w})—remain unchanged. Therefore, the equivalent parameters can be expressed as follows:

$$b_{w} = \frac{b_{e}}{(n^{o})^{2}}, \tag{1}$$

$$k_{h} = \frac{2\,(b_{e} - b_{w})^{2}\,k_{h}^{o}}{3\,(r_{e}^{o})^{2}\,F_{se}^{o}}, \tag{2}$$

and

$$k_{v} = k_{v}^{o},\ m_{v} = m_{v}^{o},\ k_{w} = k_{w}^{o}, \tag{3}$$

where the equivalent parameters, denoted as k_{h}, k_{v}, m_{v}, and k_{w}, corresponding to the original parameters k_{h}^{o}, k_{v}^{o}, m_{v}^{o}, and k_{w}^{o}, respectively. The expression for F_{se}^{o} is given by:

$$F_{se}^{o} = \frac{(n^{o})^{2}}{(n^{o})^{2} - 1}\left(\ln\frac{n^{o}}{s^{o}} + \kappa_{s}^{o}\ln s^{o} - \frac{3}{4}\right) + \left(1 - \kappa_{s}^{o}\right)\frac{(s^{o})^{2}}{(n^{o})^{2} - 1}\left[1 - \frac{(s^{o})^{2}}{4\,(n^{o})^{2}}\right] + \kappa_{s}^{o}\frac{1}{(n^{o})^{2} - 1}\left[1 - \frac{1}{4\,(n^{o})^{2}}\right], \tag{4}$$

in which $\kappa_{s}^{o} = k_{h}^{o}/k_{s}^{o}$; $n^{o} = r_{e}^{o}/r_{w}^{o}$; and $s^{o} = r_{s}^{o}/r_{w}^{o}$.

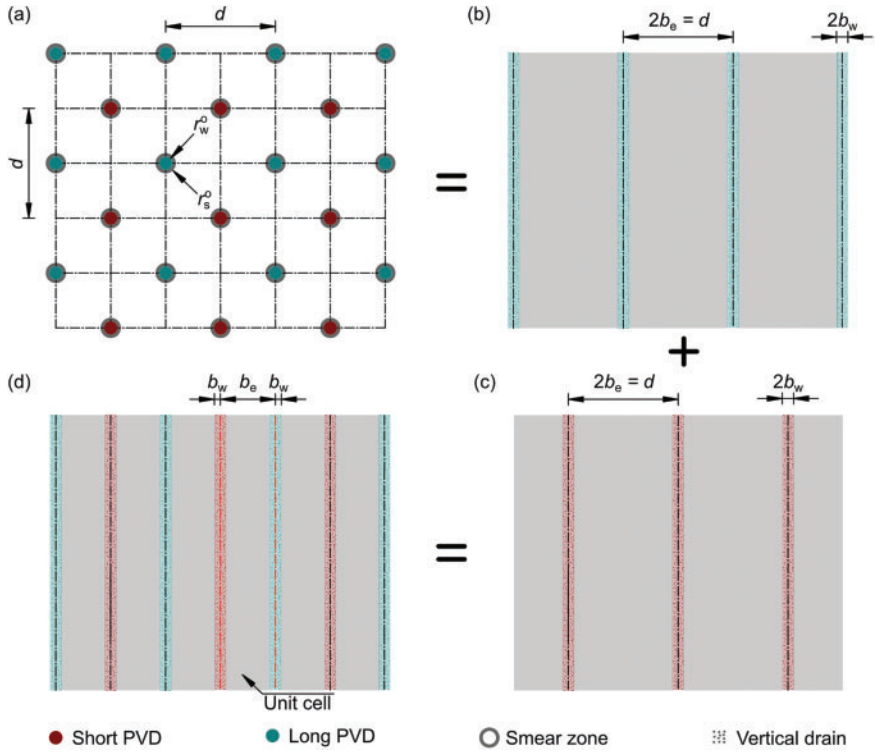

Figure 2: Schematic diagram of equivalent plane consolidation model: (a) plane layout of alternating length PVDs; (b) equivalent plane model for long PVDs; (c) equivalent plane model for short PVDs; and (d) extraction of unit cell

After obtaining the equivalent plane model as shown in Fig. 3a, the solving domain for the consolidation model becomes irregular. For simplicity, the soils below the short and long PVDs are entirely discarded, as illustrated in Fig. 3b. This approach has been demonstrated to be feasible in the consolidation analysis of ground with partially penetrating PVDs, as reported by Chen et al. [24].

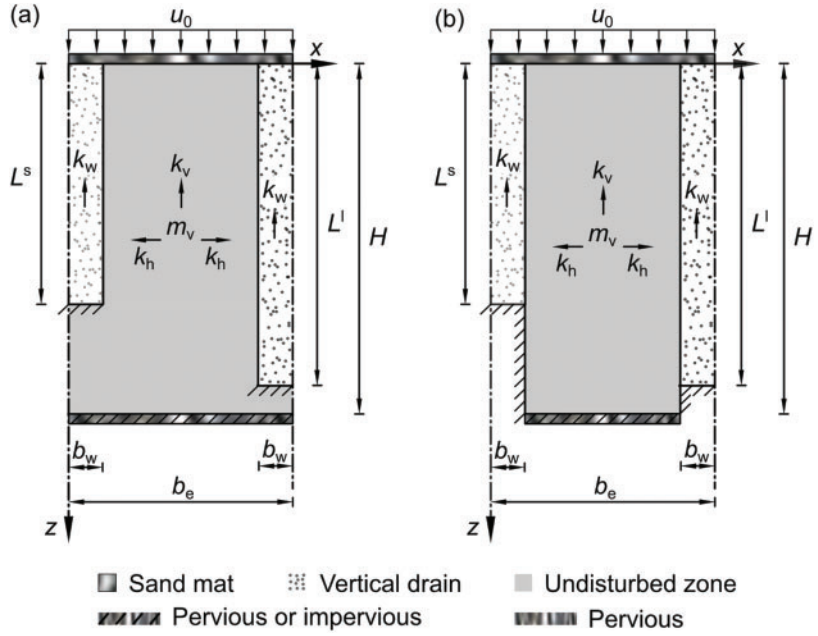

Figure 3: (a) equivalent plane consolidation model; and (b) simplified plane consolidation model

3 Equivalent Mathematical Model

3.1 Governing Equations

After model equivalence, the original three-dimensional axisymmetric consolidation model was converted into an equivalent plane model. In this model, the free-strain assumption is incorporated, whereas all other theoretical assumptions remain unchanged [24,31]. The governing equation for the equivalent plane model is given by:

$$\frac{k_h}{\gamma_w m_v}\frac{\partial^2 u}{\partial x^2}+\frac{k_v}{\gamma_w m_v}\frac{\partial^2 u}{\partial z^2}=\frac{\partial u}{\partial t},\quad (b_w \le x \le b_e - b_w), \tag{5}$$

where γ_w denotes the unit weight of water, and u is the excess pore water pressure in the soil.

According to the continuity condition of seepage flow, the difference between the vertical outflow and inflow of the drain element is equal to the amount of horizontal inflow from the surrounding foundation soil. Based on this, the seepage flow equations for the short and long PVDs are expressed as follows:

$$\frac{\partial^2 u_w^s}{\partial z^2}=-\frac{k_h}{b_w k_w}\left.\frac{\partial u}{\partial x}\right|_{x=b_w},\quad \begin{pmatrix}0 \le x \le b_w\\ 0 \le z \le L^s\end{pmatrix}, \tag{6}$$

$$\frac{\partial^2 u_w^l}{\partial z^2}=\frac{k_h}{b_w k_w}\left.\frac{\partial u}{\partial x}\right|_{x=b_e-b_w},\quad \begin{pmatrix}b_e - b_w < x \le b_e\\ 0 \le z \le L^l\end{pmatrix}, \tag{7}$$

where u_w^s and u_w^l express the excess pore pressure in short and long PVDs, respectively.

3.2 Solving Conditions

The boundary and initial conditions for the ground can be defined as follows:

$$u|_{x=b_w} = u_w^s, \quad (0 \le z \le L^s), \tag{8a}$$

$$\left.\frac{\partial u}{\partial x}\right|_{x=b_w} = 0, \quad (L^s < z \le H), \tag{8b}$$

$$u|_{x=b_e-b_w} = u_w^l, \quad \left(0 \le z \le L^l\right), \tag{9a}$$

$$\left.\frac{\partial u}{\partial x}\right|_{x=b_e-b_w} = 0, \quad \left(L^l < z \le H\right), \tag{9b}$$

$$u|_{z=0} = \left.\frac{\partial u}{\partial z}\right|_{z=H} = 0, \tag{10}$$

and

$$u|_{t=0} = u_0. \tag{11}$$

At the interfaces between the short PVD-soil and long PVD-soil, flow continuity conditions consist of two parts: continuity of excess pore pressure and flow conservation. The continuity of excess pore pressure is expressed by Eqs. (8a) and (9a), while the flow conservation condition is included in the governing equations of short and long PVDs (i.e., Eqs. (6) and (7)).

The top boundary is pervious, and the bottom boundary is impervious due to the presence of a steel plate anchor [22]. As a result, the boundary conditions for the short and long PVDs can be expressed as follows:

$$u_w^s|_{z=0} = \left.\frac{\partial u_w^s}{\partial z}\right|_{z=L^s} = 0, \tag{12}$$

and

$$u_w^l|_{z=0} = \left.\frac{\partial u_w^l}{\partial z}\right|_{z=L^l} = 0. \tag{13}$$

3.3 Normalization

To simplify the solution of the consolidation model, the following dimensionless variables are utilized:

$$X = \frac{x}{b_w},\ Z = \frac{z}{H},\ T_v = \frac{k_v t}{\gamma_w m_v H^2},\ u_D = \frac{u}{u_0},\ u_{Dw}^s = \frac{u_w^s}{u_0},\ u_{Dw}^l = \frac{u_w^l}{u_0}. \tag{14}$$

By substituting the aforementioned dimensionless variables into the governing equations and solving the conditions of the model, normalized models for the ground and PVDs can be obtained.

For the ground,

$$\kappa\eta^2\frac{\partial^2 u_D}{\partial X^2} + \frac{\partial^2 u_D}{\partial Z^2} = \frac{\partial u_D}{\partial T_v}, \quad (1 \le X \le n-1), \tag{15}$$

$$u_D|_{X=1} = u_{Dw}^s, \quad (0 \le Z \le \lambda^s), \tag{16a}$$

$$\left.\frac{\partial u_D}{\partial X}\right|_{X=1} = 0, \quad (\lambda^s < Z \le 1), \tag{16b}$$

$$u_{\mathrm{D}}|_{X=n-1} = u_{\mathrm{Dw}}^{\mathrm{l}}, \quad \left(0 \le Z \le \lambda^{\mathrm{l}}\right), \tag{17a}$$

$$\left.\frac{\partial u_{\mathrm{D}}}{\partial X}\right|_{X=n-1} = 0, \quad \left(\lambda^{\mathrm{l}} < Z \le 1\right), \tag{17b}$$

$$u_{\mathrm{D}}|_{Z=0} = 0, \tag{18}$$

$$u_{\mathrm{D}}|_{Z=1} = 0, \quad \text{(PB) or} \quad \left.\frac{\partial u_{\mathrm{D}}}{\partial Z}\right|_{Z=1} = 0, \quad \text{(IB)} \tag{19}$$

and

$$u_{\mathrm{D}}|_{T_{\mathrm{v}}=0} = 1, \tag{20}$$

where $\kappa = k_{\mathrm{h}}/k_{\mathrm{v}}$; $\eta = H/b_{\mathrm{w}}$; $n = b_{\mathrm{e}}/b_{\mathrm{w}}$; $\lambda^{\mathrm{s}} = L^{\mathrm{s}}/H$; $\lambda^{\mathrm{l}} = L^{\mathrm{l}}/H$; 'PB' represents the permeable bottom boundary; and 'IB' expresses the impermeable bottom boundary.

For short PVDs,

$$\frac{\partial^2 u_{\mathrm{Dw}}^{\mathrm{s}}}{\partial Z^2} = -\kappa_{\mathrm{w}}\eta^2 \left.\frac{\partial u_{\mathrm{D}}}{\partial X}\right|_{X=1}, \quad \begin{pmatrix} 0 \le X \le 1 \\ 0 \le Z \le \lambda^{\mathrm{s}} \end{pmatrix}, \tag{21}$$

and

$$u_{\mathrm{Dw}}^{\mathrm{s}}\big|_{Z=0} = \left.\frac{\partial u_{\mathrm{Dw}}^{\mathrm{s}}}{\partial Z}\right|_{Z=\lambda^{\mathrm{s}}} = 0. \tag{22}$$

For long PVDs,

$$\frac{\partial^2 u_{\mathrm{Dw}}^{\mathrm{l}}}{\partial Z^2} = \kappa_{\mathrm{w}}\eta^2 \left.\frac{\partial u_{\mathrm{D}}}{\partial X}\right|_{X=n-1}, \quad \begin{pmatrix} n-1 \le X \le n \\ 0 \le Z \le \lambda^{\mathrm{l}} \end{pmatrix}, \tag{23}$$

and

$$u_{\mathrm{Dw}}^{\mathrm{l}}\big|_{Z=0} = \left.\frac{\partial u_{\mathrm{Dw}}^{\mathrm{l}}}{\partial Z}\right|_{Z=\lambda^{\mathrm{l}}} = 0, \tag{24}$$

where $\kappa_{\mathrm{w}} = k_{\mathrm{h}}/k_{\mathrm{w}}$.

4 Solving Procedures

4.1 Boundary Transformation

At the lateral boundaries $X = 1$ (corresponding to Eqs. (16a) and (16b)) and $X = n - 1$ (corresponding to Eqs. (17a) and (17b)), the conditions are of a mixed-type, incorporating both Dirichlet boundaries ($0 \le Z \le \lambda^{\mathrm{s}}$ and $0 \le Z \le \lambda^{\mathrm{l}}$) and Neumann boundaries ($\lambda^{\mathrm{s}} < Z \le 1$ and $\lambda^{\mathrm{l}} < Z \le 1$). Conventional techniques, such as the method of separation of variables and the integral transform method, are not applicable for solving mathematical models under mixed-type boundary conditions [32–34]. To overcome this limitation, this study employs the boundary transform method developed by Chen et al. [35], which effectively converts the mixed boundary conditions to a unified form. The resulting transformed lateral boundary conditions at $X = 1$ and $X = n - 1$ are expressed as follows:

$$\left.\frac{\partial u_{\mathrm{D}}}{\partial X}\right|_{X=1} = \begin{cases} q^{\mathrm{s}}\left(Z, T_{\mathrm{v}}\right), & \left(0 \le Z \le \lambda^{\mathrm{s}}\right) \\ 0, & \left(\lambda^{\mathrm{s}} < Z \le 1\right) \end{cases}, \tag{25}$$

and

$$\left.\frac{\partial u_{\mathrm{D}}}{\partial X}\right|_{X=n-1}=\begin{cases}-q^{\mathrm{l}}\left(Z,T_{\mathrm{v}}\right), & \left(0\le Z\le\lambda^{\mathrm{l}}\right)\\ 0, & \left(\lambda^{\mathrm{l}}<Z\le 1\right)\end{cases}. \tag{26}$$

where $q^{\mathrm{s}}\left(Z,T_{\mathrm{v}}\right)$ and $q^{\mathrm{l}}\left(Z,T_{\mathrm{v}}\right)$ are the unknown variables that need to be determined.

It is important to emphasize that, in the above analysis, only the flow continuity conditions at the PVD-soil interfaces $X=1$ and $X=n-1$ are applied. However, the final solutions must also fulfill the pore pressure continuity conditions, as specified by Eqs. (16a) and (17a).

Incorporating Eqs. (25) and (26) into Eqs. (21) and (23), respectively, the governing equations for the short and long PVDs can be expressed as:

$$\frac{\partial^2 u_{\mathrm{Dw}}^{\mathrm{s}}}{\partial Z^2}=-\kappa_{\mathrm{w}}\eta^2 q^{\mathrm{s}}\left(Z,T_{\mathrm{v}}\right),\quad\begin{pmatrix}0\le X\le 1\\ 0\le Z\le\lambda^{\mathrm{s}}\end{pmatrix}, \tag{27}$$

and

$$\frac{\partial^2 u_{\mathrm{Dw}}^{\mathrm{l}}}{\partial Z^2}=-\kappa_{\mathrm{w}}\eta^2 q^{\mathrm{l}}\left(Z,T_{\mathrm{v}}\right),\quad\begin{pmatrix}n-1\le X\le n\\ 0\le Z\le\lambda^{\mathrm{l}}\end{pmatrix}. \tag{28}$$

4.2 Dimensionless Solutions in the Laplace Domain

To solve the ground consolidation model, a Laplace transform is first applied to the governing equation (Eq. (15)) and the boundary conditions (Eqs. (25), (26), (18), and (19)) using the initial condition specified by Eq. (20). Subsequently, a successive Fourier sine transform, followed by an inverse Fourier sine transform, is performed to derive the dimensionless excess pore pressure in the Laplace domain, expressed as follows:

$$\begin{aligned}\overline{u}_{\mathrm{D}}=&\frac{1}{p}\left\{1-\frac{\cosh\left[\sqrt{p}\left(1-Z\right)\right]}{\cosh\left(\sqrt{p}\right)}\right\}\\ &-2\sum_{m=1}^{\infty}\frac{\cosh\left[\beta_m\left(p\right)\left(n-1-X\right)\right]}{\beta_m\left(p\right)\sinh\left[\beta_m\left(p\right)\left(n-2\right)\right]}\sin\left(M_m Z\right)\int_0^{\lambda^{\mathrm{s}}}\overline{q}^{\mathrm{s}}\left(\varsigma,p\right)\sin\left(M_m\varsigma\right)d\varsigma\\ &-2\sum_{m=1}^{\infty}\frac{\cosh\left[\beta_m\left(p\right)\left(X-1\right)\right]}{\beta_m\left(p\right)\sinh\left[\beta_m\left(p\right)\left(n-2\right)\right]}\sin\left(M_m Z\right)\int_0^{\lambda^{\mathrm{l}}}\overline{q}^{\mathrm{l}}\left(\varsigma,p\right)\sin\left(M_m\varsigma\right)d\varsigma,\end{aligned} \tag{29}$$

where the Laplace domain variables corresponding to $u_{\mathrm{D}}\left(X,Z,T_{\mathrm{v}}\right)$, $q^{\mathrm{s}}\left(Z,T_{\mathrm{v}}\right)$, and $q^{\mathrm{l}}\left(Z,T_{\mathrm{v}}\right)$ are denoted as $\overline{u}_{\mathrm{D}}\left(X,Z,p\right)$, $\overline{q}^{\mathrm{s}}\left(Z,p\right)$, and $\overline{q}^{\mathrm{l}}\left(Z,p\right)$, respectively; $\beta_m\left(p\right)=\sqrt{\left(M_m^2+p\right)/\left(\kappa\eta^2\right)}$; p is the Laplace transform parameter; and $M_m=\left(2m-1\right)\pi/2$.

According to Eq. (29), the horizontal and overall average degrees of consolidation in the Laplace domain ($\overline{U}_Z$ and $\overline{U}$) can be calculated as follows:

$$\begin{aligned}\overline{U}_Z &= \frac{1}{n-2}\int_1^{n-1}\left[\frac{1}{p}-\overline{u}_{\mathrm{D}}\left(X,Z,p\right)\right]dX\\ &= \frac{\cosh\left[\sqrt{p}\left(1-Z\right)\right]}{p\cosh\left(\sqrt{p}\right)}\\ &+\frac{2}{n-2}\sum_{m=1}^{\infty}\frac{\sin\left(M_mZ\right)}{\beta_m^2\left(p\right)}\int_0^{\lambda^{\mathrm{s}}}\overline{q}^{\mathrm{s}}\left(\varsigma,p\right)\sin\left(M_m\varsigma\right)d\varsigma\\ &+\frac{2}{n-2}\sum_{m=1}^{\infty}\frac{\sin\left(M_mZ\right)}{\beta_m^2\left(p\right)}\int_0^{\lambda^{\mathrm{l}}}\overline{q}^{\mathrm{l}}\left(\varsigma,p\right)\sin\left(M_m\varsigma\right)d\varsigma,\end{aligned} \tag{30}$$

and

$$\begin{aligned}\overline{U} &= \int_0^1\overline{U}_Zdz\\ &= \frac{\tan\left(\sqrt{p}\right)}{p\sqrt{p}}+\frac{2}{n-2}\sum_{m=1}^{\infty}\frac{1-\cos\left(M_m\right)}{\beta_m^2\left(p\right)M_m}\int_0^{\lambda^{\mathrm{s}}}\overline{q}^{\mathrm{s}}\left(\varsigma,p\right)\sin\left(M_m\varsigma\right)d\varsigma\\ &+\frac{2}{n-2}\sum_{m=1}^{\infty}\frac{1-\cos\left(M_m\right)}{\beta_m^2\left(p\right)M_m}\int_0^{\lambda^{\mathrm{l}}}\overline{q}^{\mathrm{l}}\left(\varsigma,p\right)\sin\left(M_m\varsigma\right)d\varsigma.\end{aligned} \tag{31}$$

In addressing the seepage models for both short and long PVDs, a Laplace transform is initially applied to the governing equations (Eqs. (27) and (28)) as well as the vertical boundary conditions (Eqs. (22) and (24)). The transformed governing equations are then directly solved along with the corresponding vertical boundary conditions, resulting in the following expressions:

$$\overline{u}_{\mathrm{Dw}}^{\mathrm{s}}=\kappa_{\mathrm{w}}\eta^2\left[\int_0^Z\varsigma\overline{q}^{\mathrm{s}}\left(\varsigma,p\right)d\varsigma+Z\int_Z^{\lambda^{\mathrm{s}}}\overline{q}^{\mathrm{s}}\left(\varsigma,p\right)\sin d\varsigma\right], \tag{32}$$

and

$$\overline{u}_{\mathrm{Dw}}^{\mathrm{l}}=\kappa_{\mathrm{w}}\eta^2\left[\int_0^Z\varsigma\overline{q}^{\mathrm{l}}\left(\varsigma,p\right)d\varsigma+Z\int_Z^{\lambda^{\mathrm{l}}}\overline{q}^{\mathrm{l}}\left(\varsigma,p\right)\sin d\varsigma\right], \tag{33}$$

where $\overline{u}_{\mathrm{Dw}}^{\mathrm{s}}\left(Z,p\right)$ and $\overline{u}_{\mathrm{Dw}}^{\mathrm{l}}\left(Z,p\right)$ are the Laplace transformed variables of $u_{\mathrm{Dw}}^{\mathrm{s}}\left(Z,T_{\mathrm{v}}\right)$ and $u_{\mathrm{Dw}}^{\mathrm{l}}\left(Z,T_{\mathrm{v}}\right)$, respectively.

4.3 Calculation of Unknown Variables $\overline{q}^{\mathrm{s}}\left(z,p\right)$ and $\overline{q}^{\mathrm{l}}\left(z,p\right)$

The unknown variables $\overline{q}^{\mathrm{s}}\left(Z,p\right)$ and $\overline{q}^{\mathrm{l}}\left(Z,p\right)$ can be determined by applying the pore pressure continuity conditions at the PVD-soil interfaces $X=1$ and $X=n-1$. Incorporating Eqs. (29), (32), and (33) into the Laplace-transformed boundary conditions of Eqs. (16a) and (17a), it yields

$$\begin{aligned}
&\frac{1}{p}\left[1-\frac{\cosh\left[\sqrt{p}\,(1-Z)\right]}{\cosh\left(\sqrt{p}\right)}\right]\\
&=\kappa_{\mathrm{w}}\eta^{2}\left[\int_{0}^{Z}\varsigma\overline{q}^{\mathrm{s}}\left(\varsigma,p\right)d\varsigma+Z\int_{Z}^{\lambda^{\mathrm{s}}}\overline{q}^{\mathrm{s}}\left(\varsigma,p\right)d\varsigma\right]\\
&+2\sum_{m=1}^{\infty}\frac{\coth\left[\beta_{m}\left(p\right)\left(n-2\right)\right]}{\beta_{m}\left(p\right)}\sin\left(M_{m}Z\right)\int_{0}^{\lambda^{\mathrm{s}}}\overline{q}^{\mathrm{s}}\left(\varsigma,p\right)\sin\left(M_{m}\varsigma\right)d\varsigma\\
&+2\sum_{m=1}^{\infty}\frac{csch\left[\beta_{m}\left(p\right)\left(n-2\right)\right]}{\beta_{m}\left(p\right)}\sin\left(M_{m}Z\right)\int_{0}^{\lambda^{\mathrm{l}}}\overline{q}^{\mathrm{l}}\left(\varsigma,p\right)\sin\left(M_{m}\varsigma\right)d\varsigma,
\end{aligned}\tag{34}$$

and

$$\begin{aligned}
&\frac{1}{p}\left[1-\frac{\cosh\left[\sqrt{p}\,(1-Z)\right]}{\cosh\left(\sqrt{p}\right)}\right]\\
&=\kappa_{\mathrm{w}}\eta^{2}\left[\int_{0}^{Z}\varsigma\overline{q}^{\mathrm{l}}\left(\varsigma,p\right)d\varsigma+Z\int_{Z}^{\lambda^{\mathrm{l}}}\overline{q}^{\mathrm{l}}\left(\varsigma,p\right)d\varsigma\right]\\
&+2\sum_{m=1}^{\infty}\frac{csch\left[\beta_{m}\left(p\right)\left(n-2\right)\right]}{\beta_{m}\left(p\right)}\sin\left(M_{m}Z\right)\int_{0}^{\lambda^{\mathrm{s}}}\overline{q}^{\mathrm{s}}\left(\varsigma,p\right)\sin\left(M_{m}\varsigma\right)d\varsigma\\
&+2\sum_{m=1}^{\infty}\frac{\coth\left[\beta_{m}\left(p\right)\left(n-2\right)\right]}{\beta_{m}\left(p\right)}\sin\left(M_{m}Z\right)\int_{0}^{\lambda^{\mathrm{l}}}\overline{q}^{\mathrm{l}}\left(\varsigma,p\right)\sin\left(M_{m}\varsigma\right)d\varsigma.
\end{aligned}\tag{35}$$

Notably, any value of Z within the intervals $[0,\lambda^{\mathrm{s}}]$ and $\left[0,\lambda^{\mathrm{l}}\right]$ can ensure the validity of Eqs. (34) and (35).

The intervals $[0,\lambda^{\mathrm{s}}]$ and $\left[0,\lambda^{\mathrm{l}}\right]$ are evenly divided into I and J segments, respectively, each with segment lengths of ΔZ^{s} and ΔZ^{l} (as shown in Fig. 4). Within each segment, $\overline{q}^{\mathrm{s}}\left(Z,p\right)$ and $\overline{q}^{\mathrm{l}}\left(Z,p\right)$ take constant values of $\overline{q}_{i}^{\mathrm{s}}\left(p\right)(i\in[1,I])$ and $\overline{q}_{j}^{\mathrm{l}}\left(p\right)(j\in[1,J])$, respectively. Substituting the midpoint coordinates Z_{i}^{s} and Z_{j}^{l} of each segment in the intervals $[0,\lambda^{\mathrm{s}}]$ and $\left[0,\lambda^{\mathrm{l}}\right]$ into Eqs. (34) and (35), respectively, yields

$$\sum_{k=1}^{I}A_{ik}\left(p\right)\overline{q}_{k}^{\mathrm{s}}\left(p\right)+\sum_{k=1}^{J}B_{ik}\left(p\right)\overline{q}_{k}^{\mathrm{l}}\left(p\right)=a_{i}\left(p\right),\quad(1\le i\le I),\tag{36}$$

and

$$\sum_{k=1}^{I}C_{jk}\left(p\right)\overline{q}_{k}^{\mathrm{s}}\left(p\right)+\sum_{k=1}^{J}D_{jk}\left(p\right)\overline{q}_{k}^{\mathrm{l}}\left(p\right)=b_{i}\left(p\right),\quad(1\le j\le J),\tag{37}$$

where $A_{ik}\left(p\right)$, $B_{ik}\left(p\right)$, $C_{jk}\left(p\right)$, $D_{jk}\left(p\right)$, $a_{i}\left(p\right)$, and $b_{i}\left(p\right)$ can be expressed as

$$A_{ik}\left(p\right)=\kappa_{\mathrm{w}}\eta^{2}f_{ik}^{\mathrm{s}}+2\sum_{m=1}^{\infty}\frac{g_{mk}^{\mathrm{s}}}{\beta_{m}\left(p\right)}\coth\left[\beta_{m}\left(p\right)\left(n-2\right)\right]\sin\left(M_{m}Z_{i}^{\mathrm{s}}\right)$$

$$B_{ik}\left(p\right)=2\sum_{m=1}^{\infty}\frac{g_{mk}^{\mathrm{l}}}{\beta_{m}\left(p\right)}csch\left[\beta_{m}\left(p\right)\left(n-2\right)\right]\sin\left(M_{m}Z_{i}^{\mathrm{s}}\right)$$

$$C_{jk}\left(p\right)=2\sum_{m=1}^{\infty}\frac{g_{mk}^{\mathrm{s}}}{\beta_{m}\left(p\right)}csch\left[\beta_{m}\left(p\right)\left(n-2\right)\right]\sin\left(M_{m}Z_{j}^{\mathrm{l}}\right)$$

$$D_{jk}(p) = \kappa_w \eta^2 f^{l}_{jk} + 2\sum_{m=1}^{\infty} \frac{g^{l}_{mk}}{\beta_m(p)} \coth\left[\beta_m(p)(n-2)\right] \sin\left(M_m Z^{l}_j\right)$$

$$a_i(p) = \left\{1 - \cosh\left[\sqrt{p}\left(1 - Z^{s}_i\right)\right] / \cosh\left(\sqrt{p}\right)\right\} / p$$

$$b_i(p) = \left\{1 - \cosh\left[\sqrt{p}\left(1 - Z^{l}_j\right)\right] / \cosh\left(\sqrt{p}\right)\right\} / p,$$

in which

$$f^{s}_{ik} = \begin{cases} \Delta Z^{s}_k Z^{s}_k, & 1 \le k \le i-1 \\ \Delta Z^{s}_i \left(Z^{s}_i - \frac{\Delta Z^{s}_i}{8}\right), & k = i \\ \Delta Z^{s}_k Z^{s}_i, & i+1 \le k \le I \end{cases}$$

$$f^{l}_{ik} = \begin{cases} \Delta Z^{l}_k Z^{l}_k, & 1 \le k \le j-1 \\ \Delta Z^{l}_j \left(Z^{l}_j - \frac{\Delta Z^{l}_j}{8}\right), & k = j \\ \Delta Z^{l}_k Z^{l}_j, & j+1 \le k \le J \end{cases}$$

$$g^{s}_{mk} = \frac{2}{M_m} \sin\left(M_m Z^{s}_k\right) \sin\left(\frac{M_m \Delta Z^{s}_k}{2}\right)$$

$$g^{l}_{mk} = \frac{2}{M_m} \sin\left(M_m Z^{l}_k\right) \sin\left(\frac{M_m \Delta Z^{l}_k}{2}\right).$$

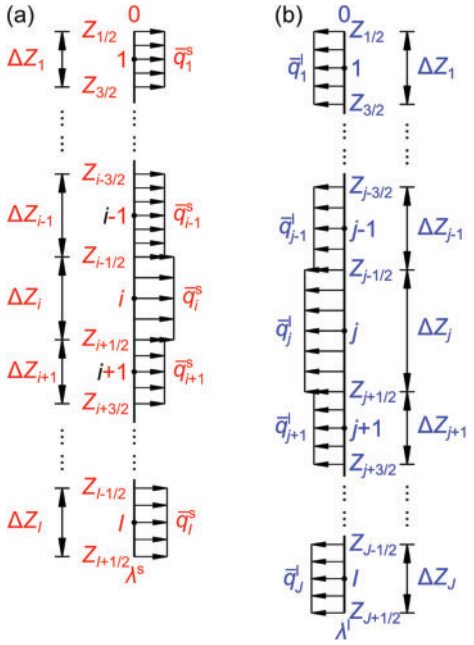

Figure 4: Local discretization of (a) short PVD-soil interface, and (b) long PVD-soil

To solve $\overline{q}^{s}_i(p)(i = 1, 2, \ldots, I)$ and $\overline{q}^{l}_j(p)(j = 1, 2, \ldots, J)$ efficiently, Eqs. (36) and (37) are reformulated in matrix form as

$$\begin{bmatrix} \mathbf{A}_{I\times I} & \mathbf{B}_{I\times J} \\ \mathbf{C}_{J\times I} & \mathbf{D}_{J\times J} \end{bmatrix} \begin{Bmatrix} \overline{\mathbf{q}}^{\mathrm{s}}_{I\times 1} \\ \overline{\mathbf{q}}^{\mathrm{l}}_{J\times 1} \end{Bmatrix} = \begin{Bmatrix} \mathbf{a}_{I\times 1} \\ \mathbf{b}_{J\times 1} \end{Bmatrix}, \tag{38}$$

where matrices $\mathbf{A}_{I\times I}$, $\mathbf{B}_{I\times J}$, $\mathbf{C}_{J\times I}$, and $\mathbf{D}_{J\times J}$ are composed of elements $A_{ik}(p)$, $B_{ik}(p)$, $C_{jk}(p)$, and $D_{jk}(p)$, respectively; $\overline{\mathbf{q}}^{\mathrm{s}}_{I\times 1} = \left[\overline{q}^{\mathrm{s}}_1(p) \quad \dots \quad \overline{q}^{\mathrm{s}}_I(p)\right]^{\mathrm{T}}$; $\overline{\mathbf{q}}^{\mathrm{l}}_{J\times 1} = \left[\overline{q}^{\mathrm{l}}_1(p) \quad \dots \quad \overline{q}^{\mathrm{l}}_J(p)\right]^{\mathrm{T}}$; $\mathbf{a}_{I\times 1} = \left[a_1(p) \quad \dots \quad a_I(p)\right]^{\mathrm{T}}$; and $\mathbf{b}_{J\times 1} = \left[b_1(p) \quad \dots \quad b_J(p)\right]^{\mathrm{T}}$.

Once the discrete variables $\overline{q}^{\mathrm{s}}_i(p)$ $(i = 1, 2, \dots, I)$ and $\overline{q}^{\mathrm{l}}_j(p)$ $(j = 1, 2, \dots, J)$ are obtained and incorporated into Eqs. (29)∼(33), the Laplace domain solutions for the ground consolidation and the seepage models of both short and long PVDs are obtained. These solutions can then be transformed into the time domain through the application of a numerical Laplace inversion technique [36].

5 Numerical Verification

The proposed solutions are derived using the model equivalence technique, boundary transform method, and local discretization method. Additionally, the soils below short and long PVDs are assumed to be discarded to form a regular solving domain. While the previous subsection mainly focuses on the accuracy evaluation of the equivalent plane model, this subsection employs numerical analysis to comprehensively investigate the effectiveness of the measures adopted in the model equivalence and solving procedures.

To simplify the simulation process based on the symmetry of PVDs' layout, a unit cell presented in Fig. 5 is selected, and the parameters used in the numerical calculation are listed in Table 1. The Heat Transfer interface within the Mathematics Module of COMSOL Multiphysics is employed to simulate soil consolidation. The governing equation is as follows:

$$d_{\mathrm{a}}\frac{\partial u}{\partial t} + \nabla \cdot (-c\nabla u) = f, \tag{39}$$

where u denotes the temperature variable, representing the excess pore pressure in the consolidation model; d_{a} is the damping or mass coefficient, corresponding to $\gamma_{\mathrm{w}} m_{\mathrm{v}}$ in the consolidation model; c is the diffusion coefficient, representing the coefficient of permeability; and f is the source term, which is set to zero in the consolidation model. It should be noted that the seepage within both the short and long PVDs is also simulated using Eq. (39), with the mass coefficient d_{a} set to a very small value (taken as $10^{-10}\,\mathrm{m}^{-1}$ in this model) to represent the assumption that seepage occurs without deformation in the PVDs. The solving conditions are the same as the original model.

By utilizing the model equivalence technique, the equivalent parameters of the simplified model are determined as follows: $k_{\mathrm{h}} = 1.703 \times 10^{-9}$ m/s, $k_{\mathrm{v}} = 10^{-8}$ m/s, $k_{\mathrm{w}} = 10^{-5}$ m/s, $m_{\mathrm{v}} = 5 \times 10^{-7}\,\mathrm{Pa}^{-1}$, $b_{\mathrm{w}} = 9.817 \times 10^{-4}$ m, and $b_{\mathrm{e}} = 5 \times 10^{-1}$ m. The other parameters not listed above remain the same as those in the original model. The original model and the equivalent model are calculated using the finite element method and the method proposed in this paper, respectively. Fig. 6 compares the overall average degree of consolidation obtained by the proposed method and the numerical method. The agreement between the numerical solution and the proposed solution is reasonable, indicating that the equivalent plane model can effectively replace the original three-dimensional model, and all measures used to solve the equivalent model are feasible. It should be mentioned that the influence of discarding the soil below short and long PVDs on the overall consolidation degree of the ground can be ignored, which is consistent with the free strain consolidation model of ground with partially penetrating PVDs proposed by Chen et al. [24]. This conclusion provides a novel idea for solving the equal strain consolidation model with partially penetrating or long-short vertical drains, thereby avoiding the complexity of traditional methods [37].

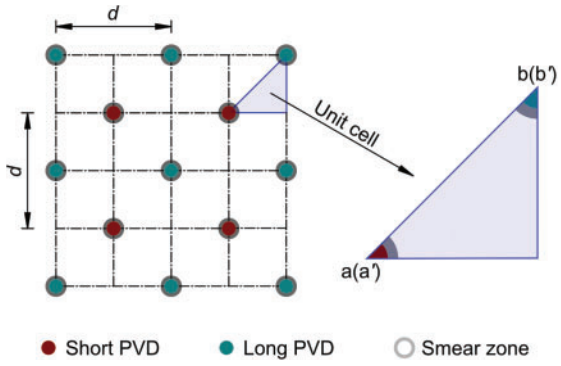

Figure 5: Unit cell extraction for numerical calculation

Table 1: Calculation parameters of the numerical model

Parameter	Value
r_w^o	2.5 cm
r_s^o	5 cm
d	1 m
L^s	10 m
L^l	15 m
k_w^o	10^{-5} m/s
H	20 m
$k_h^o = k_v^o$	10^{-8} m/s
k_s^o	5×10^{-9} m/s
m_v^o	5×10^{-7} Pa^{-1}
σ	100 kPa

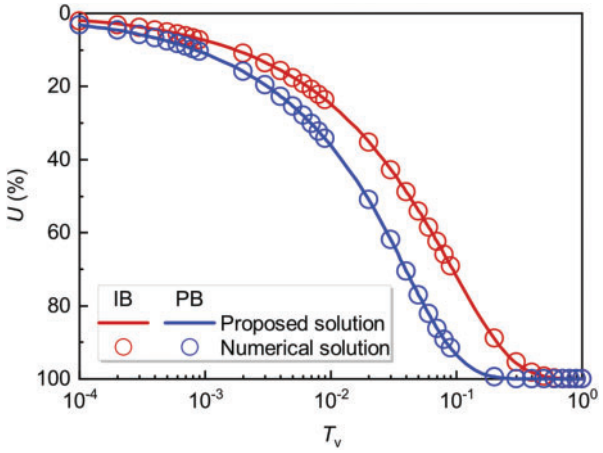

Figure 6: Comparison of proposed and numerical solutions for IB and PB conditions

6 Influence of Penetration Depth of PVDs

To facilitate the implementation of ground improvement with alternating length PVDs, it is necessary to investigate the impact of penetration depth on consolidation characteristics. All the parameters used in the analyses are identical to those in Table 1, except for the investigated parameters L^s and L^l. Furthermore, only the 'PB' condition is considered below. The influence of the penetration depth of alternating PVDs is divided into two categories: inconstant and constant total length of PVDs.

6.1 Inconstant $\lambda^s + \lambda^l$

For comparison, four different dimensionless penetration depths of short PVDs (i.e., $\lambda^s = 0.4$, 0.6, 0.8, and 1.0) are utilized, while long PVDs are installed to the full depth of the ground (i.e., $\lambda^l = 1.0$). As depicted in Fig. 7, the influence of the penetration depth of PVDs during the early stage of consolation can be disregarded, as the four consolidation curves nearly coincide. This is attributed to the fact that, during the early stage of consolidation, consolidation mainly occurs in the upper soil layer, rendering the effect of increasing the short PVDs length on consolidation efficiency minimal. During the middle and later stages of consolidation, increasing the penetration depth of short PVDs gradually improves consolidation efficiency. However, the accompanying increase in well resistance limits the effectiveness of further extending the short PVDs, thereby reducing the marginal improvement in consolidation efficiency. For instance, when $U = 80\%$, the required consolidation time for $\lambda^s = 0.4$, 0.6, 0.8, and 1.0 are $T_v = 0.137$, 0.122, 0.116, and 0.115, respectively. That is to say, the penetration depth of short PVDs can be reduced up to $0.6\,H$ without any significant increase in the consolidation time for $U = 80\%$, which is consistent with the conclusion proposed by Indraratna and Rujikiatkamjorn [38].

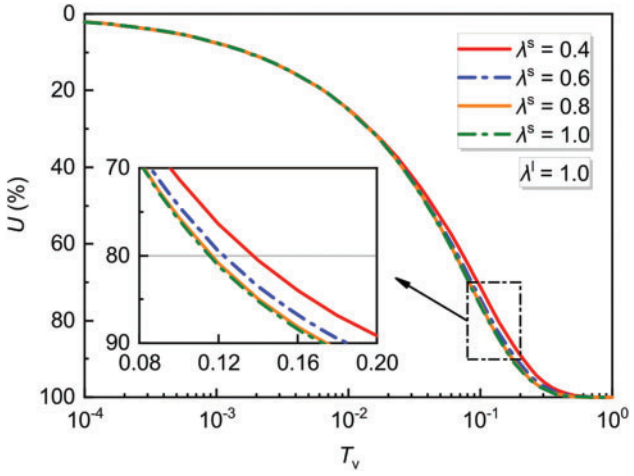

Figure 7: Overall average degree of consolidation for different penetration depths of short PVDs (inconstant $\lambda^s + \lambda^l$, but fixed $\lambda^l = 1.0$)

6.2 Constant $\lambda^s + \lambda^l$

To investigate the effect of penetration depth of PVDs on consolidation under a given total length (i.e., $\lambda^s + \lambda^l = 1.2$), four different penetration depths of short PVDs (i.e., $\lambda^s = 0.2$, 0.3, 0.4, and 0.6) are considered, and the results are given in Fig. 8. The consolidation characteristic under different lengths of short PVDs is found to be very complicated, with intersections between different consolidation curves. Taking the consolidation curves corresponding to $\lambda^s = 0.4$ and $\lambda^s = 0.6$ as an example, the

overall average of consolidation for $\lambda^s = 0.6$ is larger than that for $\lambda^s = 0.4$ before the time factor $T_v = 0.085$, whereas an opposite conclusion can be drawn after this point.

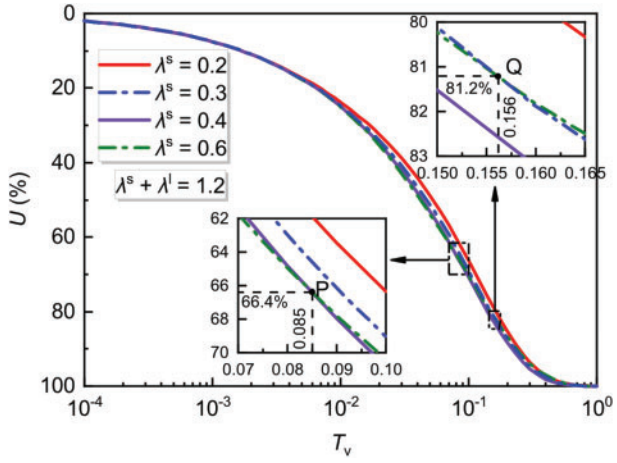

Figure 8: Overall average degree of consolidation for different penetration depths of short PVDs (constant $\lambda^s + \lambda^l = 1.2$)

To intuitively show the influence of penetration depth of alternating length PVDs on consolidation characteristics, the variations of consolidation time required to achieve a given consolidation degree are shown in Fig. 9. The results indicate that the time needed to reach a specific consolidation degree first decreases and then increases with the penetration depth of short PVDs. There exists an optimal penetration depth for short PVDs, which corresponds to the minimum time factor. Notably, the optimal penetration depth of PVDs is not $\lambda^s = \lambda^l = 0.6$, suggesting that alternating length PVDs are more effective than equal length PVDs. Moreover, as the desired consolidation degree increases, the layout of PVDs deviates from the equal length layout, with the optimal length of short PVDs decreasing. For example, the optimal penetration depths of short PVDs for $U = 50\%$, 60%, 70%, 80%, and 90%, are $\lambda^s = 0.550$, 0.515, 0.480, 0.450, and 0.425, respectively.

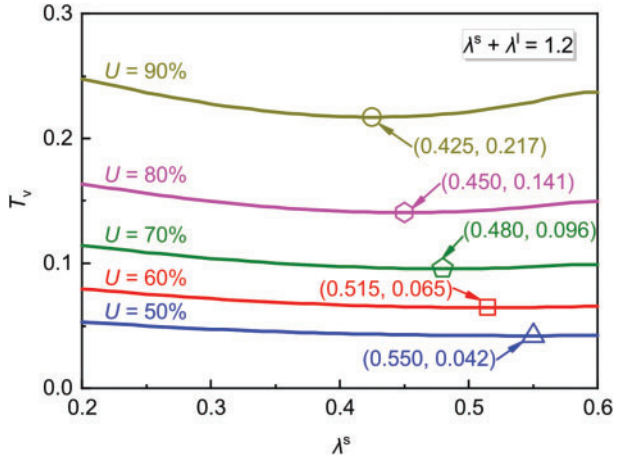

Figure 9: Consolidation time required to reach different overall average degrees of consolidation (constant $\lambda^s + \lambda^l = 1.2$)

In practice, it is often unnecessary for the entire soft soil layer to reach the designed strength when the ground thickness is substantial. Construction can be carried out if the soil above a design depth meets the required strength criteria. Given this, the consolidation characteristics of the ground with alternating length PVDs vs. equal length PVDs are compared, using the average degree of consolidation U_u within the design depth H_d and the average degree of consolidation U_d below the design depth H_d, which can be expressed as:

$$U_u(T_v) = \frac{1}{\lambda_d}\int_0^{\lambda_d} U_Z(T_v)\,dZ, \tag{40}$$

and

$$U_d(T_v) = \frac{1}{1-\lambda_d}\int_{\lambda_d}^{1} U_Z(T_v)\,dZ, \tag{41}$$

where $\lambda_d = H_d/H$.

The scheme of alternating length PVDs is more adaptive than the layout of equal length PVDs for a given total length of PVDs. A control case with equal length PVDs is considered, and the design average degrees of consolidation within the design depth $\lambda_d = 0.8$, corresponding to the time factors $T_v = 0.109$, 0.144, and 0.194, are $U_u = 80\%$, 85%, and 90%, respectively. To ensure that the ground improved with alternating length PVDs also reaches the design average degree of consolidation at the same time point, the consolidation model is back-calculated to obtain the length of short PVDs. The resulting average degrees of consolidation within and below the design depth (i.e., U_u and U_d) are presented in Fig. 10. The results show that the consolidation of the ground with alternating length PVDs is faster than that of the ground with equal length PVDs after reaching the design consolidation degree. Furthermore, for the ground with alternating length PVDs, the average degree of consolidation below the design depth is higher than that of the ground with equal length PVDs when the average degree of consolidation within the design depth reaches the target value. For example, when the U_u value reaches 80%, 85%, and 90%, the U_d value for alternating length PVDs can be increased by 5.30%, 7.42%, and 7.27%, respectively, compared to the case with equal length PVDs. Overall, the layout of PVDs with alternating length is superior to that of equal-length PVDs when the total length of PVDs remains constant.

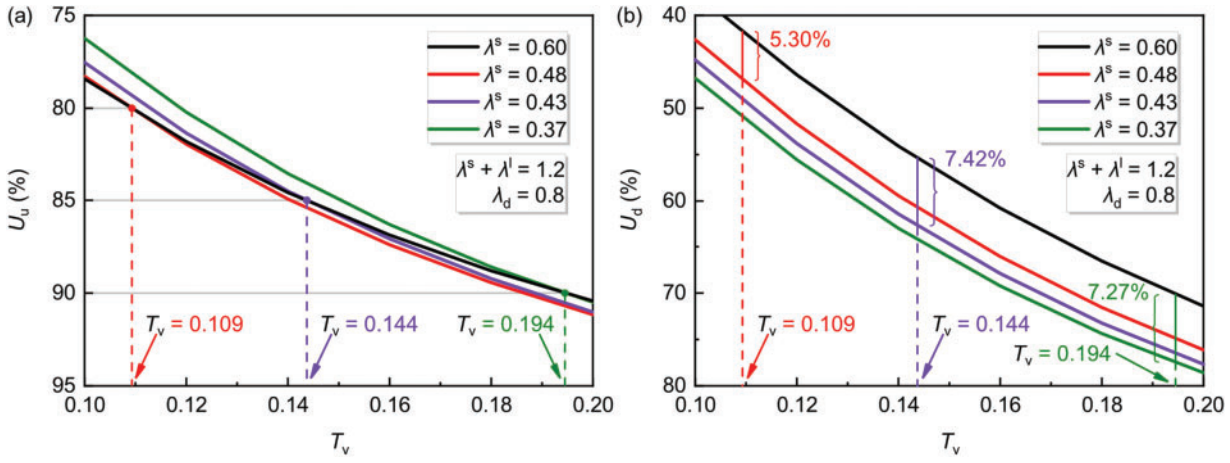

Figure 10: Average degree of consolidation (a) within the design depth; and (b) below the design depth for different penetration depths of short PVDs (constant $\lambda^s + \lambda^l = 1.2$)

7 Conclusions

This paper proposes an equivalent plane model to describe the free strain consolidation of ground with alternating length PVDs. A semi-analytical solution for this equivalent plane model is derived using the boundary transform and local discretization methods. The effectiveness of the solution is evaluated, and a parametric study is conducted to assess the influence of the penetration depth of short and long PVDs on the consolidation behavior. The main conclusions of the study are as follows:

1. The model equivalence technique is effective in simplifying the original three-dimensional model into an equivalent plane model, in which the soil below short and long PVDs can be discarded to have a negligible impact on the overall average degree of consolidation, and as such, measures used to solve the equivalent plane model become feasible.
2. There are intersections between the consolidation curves for the ground with equal length and alternating length PVDs. The overall average degree of consolidation for alternating length PVDs is less than that for equal length PVDs before reaching the intersection, whereas an opposite conclusion is achieved after passing the intersection.
3. When the total length of PVDs is constant, the time needed to reach a given consolidation degree firstly decreases, and then increases with the penetration depth of short PVDs. The optimal penetration depth of short PVDs, corresponding to the minimum time factor, is not consistent with the case of equal length PVDs, which decreases with the increase of design consolidation degree. Besides, the average degrees of consolidation within and below the design depth for alternating length PVDs are faster than those for equal length PVDs after the soil within the design depth reaches the target consolidation degree.

Acknowledgement: The authors are grateful to all the editors and anonymous reviewers for their comments and suggestions.

Funding Statement: The authors appreciate the financial support provided by the National Natural Science Foundation of China (Grant No. 52408358), the Natural Science Foundation of Hainan Province (Grant Nos. 523QN213 and 524RC476), the Systematic Project of Guangxi Key Laboratory of Disaster Prevention and Engineering Safety (Grant No. 2022ZDK008), the Scientific Research Foundation of Hainan Key Laboratory of Marine Geological Resources and Environment (Grant No. HNHYDZZYHJKF040), and the Scientific Research Foundation of Hainan University (Nos. KYQD(ZR)-21067 and RZ2200001147).

Author Contributions: The authors confirm contribution to the paper as follows: Conceptualization: Bowen Lv, Chen Zhang, and Zheng Chen; methodology: Chen Zhang, Weihong Zhou, Hao Wang, and Zheng Chen; software: Bowen Lv, Weihong Zhou, and Fei Wang; validation: Chen Zhang, Weihong Zhou, Hao Wang, and Fei Wang; analysis and interpretation of results: Bowen Lv and Zheng Chen; supervision: Zheng Chen; funding acquisition: Zheng Chen. All authors reviewed the results and approved the final version of the manuscript.

Availability of Data and Materials: The data that support the findings of this study are available from the corresponding author, Zheng Chen, upon reasonable request.

Ethics Approval: Not applicable.

Conflicts of Interest: The authors declare no known competing financial interests or personal relationships that could have appeared to influence the work reported in this paper.

Supplementary Materials: The supplementary material is available online at https://doi.org/10.23967/j.rimni.2025.10.65700.

References

1. Sun L, Gao X, Zhuang D, Guo W, Hou J, Liu X. Pilot tests on vacuum preloading method combined with short and long PVDs. Geotextiles Geomembr. 2018;46:243–50. doi:10.1016/j.geotexmem.2017.11.010.
2. Barron RA. Consolidation of fine-grained soils by drain wells. Trans Am Soc Civil Eng. 1948;113:718–42. doi:10.1061/taceat.0006098.
3. Hansbo S. Consolidation of fine-grained soils by prefabricated drains. In: Proceedings 10th International Conference Soil Mechanics and Found Engineering; 1981 Jun 15–19; Stockholm: International Society of Soil Mechanics and Foundation Engineering. Vol. 3, p. 677–82.
4. Xie K, Zeng G. Consolidation theories for drain wells under equal strain condition. Chin J Geotech Eng. 1989;2:3–17.
5. Chai JC, Fu HT, Wang J, Shen SL, Ding W. Method for calculating cyclic load induced 1D and PVD unit cell consolidation deformations. Comput Geotech. 2021;136:104243. doi:10.1016/j.compgeo.2021.104243.
6. Liu J, Lei G, Zheng M. General solutions for consolidation of multilayered soil with a vertical drain system. Geotextiles Geomembr. 2014;42:267–76. doi:10.1016/j.geotexmem.2014.04.001.
7. Sun J, Lu M, Yang K, Han B. Nonlinear consolidation analysis for composite ground with combined use of impervious columns and prefabricated vertical drains under time-dependent loading. Comput Geotech. 2023;161:105563. doi:10.1016/j.compgeo.2023.105563.
8. Zhou Y, Sun L, Ren Y. Consolidation analyses of PVD-improved marine clay considering long-term natural sedimentation. Appl Ocean Res. 2023;141:103795.
9. Tang X, Niu B, Cheng G, Shen H. Closed-form solution for consolidation of three-layer soil with a vertical drain system. Geotextiles Geomembr. 2013;36:81–91. doi:10.1016/j.geotexmem.2012.12.002.
10. Tang XW, Onitsuka K. Consolidation of double-layered ground with vertical drains. Int J Numer Anal Methods Geomech. 2001;25:1449–65. doi:10.1002/nag.191.
11. Yin JH, Chen ZJ, Feng WQ. A general simple method for calculating consolidation settlements of layered clayey soils with vertical drains under staged loadings. Acta Geotechnica. 2022;17:3647–74. doi:10.1007/s11440-021-01318-2.
12. Deng Y-B, Xie K-H, Lu M-M. Consolidation by vertical drains when the discharge capacity varies with depth and time. Comput Geotech. 2013;48:1–8. doi:10.1016/j.compgeo.2012.09.012.
13. Deng Y-B, Xie K-H, Lu M-M, Tao H-B, Liu G-B. Consolidation by prefabricated vertical drains considering the time dependent well resistance. Geotextiles Geomembr. 2013;36:20–6. doi:10.1016/j.geotexmem.2012.10.003.
14. Lu X, Li C, Wang P. An analytical solution for nonlinear consolidation of composite foundations improved by impermeable columns and vertical drains with time-dependent well resistance. Int J Geomech. 2024;24:06024017. doi:10.1061/ijgnai.gmeng-9464.
15. Indraratna B, Zhong R, Fox PJ, Rujikiatkamjorn C. Large-strain vacuum-assisted consolidation with non-Darcian radial flow incorporating varying permeability and compressibility. J Geotech Geoenviron Eng. 2017;143:04016088. doi:10.1061/(asce)gt.1943-5606.0001599.
16. Pu H, Yang P, Lu M, Zhou Y, Chen JN. Piecewise-linear large-strain model for radial consolidation with non-Darcian flow and general constitutive relationships. Comput Geotech. 2020;118:103327. doi:10.1016/j.compgeo.2019.103327.

17. Walker R, Indraratna B, Rujikiatkamjorn C. Vertical drain consolidation with non-Darcian flow and void-ratio-dependent compressibility and permeability. Géotechnique. 2012;62:985–97. doi:10.1680/geot.10.p.084.
18. Xu C, Liu Z, Zhang J, Huang J. Analysis of large-strain elastic viscoplastic consolidation for soft clay with vertical drains considering non-Darcian flow. Appl Math Model. 2021;92:770–84. doi:10.1016/j.apm.2020.11.038.
19. Wang Y, Li C. Large strain consolidation of soft soils with partially penetrating PVDs: analytical solutions incorporating variable well resistance. Comput Geotech. 2024;174:106600. doi:10.1016/j.compgeo.2024.106600.
20. Guo W, Zhou Y, Sun L, Jiang H, Lang R, Chen H, et al. Large-strain consolidation of vacuum preloading combined with partially penetrating prefabricated vertical drains. Int J Numer Anal Methods Geomech. 2024;48:2450–67. doi:10.1002/nag.3736.
21. Hart E, Kondner R, Boyer W. Analysis for partially penetrating sand drains. J Soil Mech Foundations Div. 1958;84(4). doi:10.1061/jsfeaq.0000139.
22. Nghia NT, Lam LG, Shukla SK. A new approach to solution for partially penetrated prefabricated vertical drains. Int J Geosynth Ground Eng. 2018;4:11. doi:10.1007/s40891-018-0128-8.
23. Wang XS, Jiao JJ. Analysis of soil consolidation by vertical drains with double porosity model. Int J Numer Anal Methods Geomech. 2004;28:1385–400. doi:10.1002/nag.391.
24. Chen Z, Ni P, Mei G, Chen Y. Semi-analytical solution for consolidation of ground with partially penetrating PVDs under the free-strain condition. J Eng Mech. 2021;147:04020148. doi:10.1061/(asce)em.1943-7889.0001884.
25. Liu J, Shi J. An equivalent calculation method to converse vertical drains foundation into vertical walls foundation. Rock Soil Mech. 2004;25:1782–5.
26. Nguyen B-P, Yun D-H, Kim Y-T. An equivalent plane strain model of PVD-improved soft deposit. Comput Geotech. 2018;103:32–42. doi:10.1016/j.compgeo.2018.07.004.
27. Tran TA, Mitachi T. Equivalent plane strain modeling of vertical drains in soft ground under embankment combined with vacuum preloading. Comput Geotech. 2008;35:655–72. doi:10.1016/j.compgeo.2007.11.006.
28. Chai J, Bergado DT, Shen S-L. Modelling prefabricated vertical drain improved ground in plane strain analysis. Proc Inst Civil Eng-Ground Impr. 2013;166:65–77. doi:10.1680/grim.11.00007.
29. Indraratna B, Sathananthan I, Rujikiatkamjorn C, Balasubramaniam A. Analytical and numerical modeling of soft soil stabilized by prefabricated vertical drains incorporating vacuum preloading. Int J Geomech. 2005;5:114–24. doi:10.1061/(asce)1532-3641(2005)5:2(114).
30. Nghia-Nguyen T, Shukla SK, Dang PH, Lam L, Khatir S, Cuong-Le T. Numerical modeling of prefabricated vertical drain with vacuum consolidation technique. Transp Infrastruct Geotechnol. 2021;9:1–17. doi:10.1007/s40515-021-00165-8.
31. Leo CJ. Equal strain consolidation by vertical drains. J Geotech Geoenviron Eng. 2004;130:316–27. doi:10.1061/(asce)1090-0241(2004)130:3(316).
32. Chen Z, Ni P, Chen Y, Mei G. Plane-strain consolidation theory with distributed drainage boundary. Acta Geotechnica. 2020;15:489–508. doi:10.1007/s11440-018-0712-z.
33. Wang Q, Zhan H. The effect of intra-wellbore head losses in a vertical well. J Hydrol. 2017;548:333–41. doi:10.1016/j.jhydrol.2017.02.042.
34. Wang S, Ni P, Chen Z, Mei G. Consolidation solution of soil around a permeable pipe pile. Marine Georesources Geotechnol. 2020;38:1097–105.
35. Chen Z, Ni P, Zhu X, Mei G. Using boundary transform method to solve geotechnical problems with mixed-type boundary conditions. J Geotech Geoenviron Eng. 2022;148:06022013. doi:10.1061/(asce)gt.1943-5606.0002921.

36. Durbin F. Numerical inversion of Laplace transforms: an efficient improvement to Dubner and Abate's method. Comput J. 1974;17:371–6. doi:10.1093/comjnl/17.4.371.
37. Geng X, Indraratna B, Rujikiatkamjorn C. Effectiveness of partially penetrating vertical drains under a combined surcharge and vacuum preloading. Can Geotech J. 2011;48:970–83. doi:10.1139/t11-011.
38. Indraratna B, Rujikiatkamjorn C. Effects of partially penetrating prefabricated vertical drains and loading patterns on vacuum consolidation. In: GeoCongress 2008: Geosustainability and Geohazard Mitigation; 2008. Vol. 29, p. 596–603. doi:10.1061/40971(310)74.